J Mater Sci (2019) 54:14897–14904

Materials for life sciences

Ultra-long ZnO/carbon nanofiber as free-standing electrochemical sensor for dopamine in the presence of uric acid

Chi Yang[1,2,*], Chunyan Zhang[1], Tong Huang[1], Xiuxiu Dong[2], and Langqin Hua[1]

[1] Yale-NUIST Center on Atmospheric Environment, International Joint Laboratory on Climate and Environment Change (ILCEC), School of Applied Meteorology, Nanjing University of Information Science and Technology, Nanjing 210044, China
[2] State Key Laboratory of Bioelectronics, School of Biological Science and Medical Engineering, Southeast University, Nanjing 210096, China

Received: 27 June 2019
Accepted: 4 September 2019
Published online: 9 September 2019

ABSTRACT

Dopamine (DA) and uric acid (UA) have similar peak potentials in vivo, and it is difficult to distinguish them by general electrode material. Here, we used a magnetron sputtering method to sputter the ZnO seed layer on carbon fiber and prepare ultra-long ZnO nanofibers/carbon fibers (ZnO NF/CF) electrode by in situ hydrothermal method. As a free-standing electrode, not only electrochemical detection of DA and UA but also a separation of oxidation potential peaks of DA and UA can be achieved. In addition, in the case of high concentration UA (0.1 mM), ZnO NF/CF shows high sensitivity and selectivity and shows a wide linear range for DA (4–20 μM). Meanwhile, we proposed the electrochemical mechanism and process of DA and UA on the surface of ZnO, which helps us to understand the simultaneous detection of DA and UA by such electrochemical electrodes.

Introduction

Ultra-long nanofibers with large anisotropy can be used in many fields such as composites, microelectronics, separation, and biosensing [1, 2]. Among them, ZnO nanofibers are widely used in sensors due to their high sensitivity, low detection limit, and fast electron transfer kinetics [3–6]. At present, electrospinning and sol–gel, combined with magnetron sputtering methods, are widely used for preparing ultra-long nanofibers, and hydrothermal growth methods using carbon fibers as a template are also included [7, 8]. These preparation methods result in ordered ultra-long nanofibers to further achieve the desired function [9, 10]. The carbon fiber here is chemically resistant and electrically conductive and is often used as the electrode material [11] in addition to being used as a template. Therefore, the carbon fiber and the nanomaterial grown thereon can be

Address correspondence to E-mail: yangchi@seu.edu.cn

https://doi.org/10.1007/s10853-019-04000-x

directly served as an unsupported electrode which does not require a commercial electrode as support [12–15]. Yang [3] used this type of electrode to achieve the detection of dopamine, and Liu [16] achieved simultaneous detection of uric acid and ascorbic acid.

The detection of dopamine (DA) is of great significance for the diagnosis of neurological diseases such as schizophrenia and Parkinson's disease [17]. However, the current electrochemical detection of DA is disturbed because uric acid (UA) and DA have similar redox potentials in vivo [18]. The solution to this problem is usually to use a modified electrode so that the redox potentials of the two do not overlap. At present, complex of cyclodextrin and graphene [19, 20], precious metal composite [21–24], inorganic compound boron nitride [25], semiconductor composite indium tin oxides [26], graphene composite [27, 28], and electrochemically pretreated pencil graphite electrodes [29], these material modification electrodes have achieved a distinction for the oxidation–reduction potential of UA and DA.

Inspired by the above work, we sputtered ZnO seed layer on carbon fiber and prepared ZnO nanofibers/carbon fibers (ZnO NF/CF) free-standing electrodes by hydrothermal method. The vision is to use this electrode to distinguish the oxidative–reduction potentials of UA and DA while achieving their simultaneous detection.

Experiment

Reagent

DA and UA were purchased from Sigma-Aldrich. Different pH phosphate, buffer solutions (PBS) were prepared by mixing NaH_2PO_4 and Na_2HPO_4 solutions and then adjusting the pH with 0.1 M NaOH and H_3PO_4. All other chemicals are of analytical grade and are used as received. All solutions were prepared using ultra-pure water (≥ 18 MΩ, Milli-Q, Millipore). The DA hydrochloride and UA solutions were prepared on the same day and stored in the refrigerator.

Instrument

Scanning electron microscopy (SEM, JSM-6330F) and energy-dispersive spectroscopy (EDS) were used to measure the surface morphology, and elemental analysis was performed on the sample. The X-ray diffraction pattern was obtained using XRD-6000 diffracted radiation (Cu K, λ = 0.15406 nm).

Electrochemical measurements of cyclic voltammetry (CV) and differential pulse voltammetry (DPV) were performed using a CHI 660E workstation (Shanghai Chenhua Instrument Corporation, China). CV experiments were performed at a scan rate of 50 mV s^{-1} unless otherwise stated. The DPV experiment was performed with the following parameters: amplitude, 0.05 V; pulse width, 0.2 s; sample width, 0.0167 s; pulse period, 0.5 s; and quiet time, 2 s.

Preparation of ultra-long ZnO NF/CF electrode

The ultra-long ZnO NF/CF free-standing electrode was obtained in two steps, as shown in Scheme 1; the first step is to sputter a ZnO seed layer on the surface of the carbon fiber by RF magnetron sputtering (MSP-30 °C). Briefly, a ZnO (5 N, 7.5 cm diameter) target was used to deposit a ZnO layer (length and diameter of 4 cm and 2 mm, respectively) on a carbon fiber substrate. A gas mixture of Ar (50%) and N_2 (10%) having a total pressure of 1.0 Pa was used as a sputtering gas. All samples were sprayed for 5 min under conditions of 3.3 Pa, 50 sccm Ar, and 10 sccm N_2. Next, a mixed solution of zinc acetate dihydrate (0.05 M) and hexamethylenetetramine (HMTA, 0.05 M) was prepared, and after stirring for 5 min, it was transferred to a Teflon lined stainless steel autoclave having a volume of 50 mL. Carbon fibers sputtered with a ZnO seed layer were immersed in the above-mixed solution. The mixture was

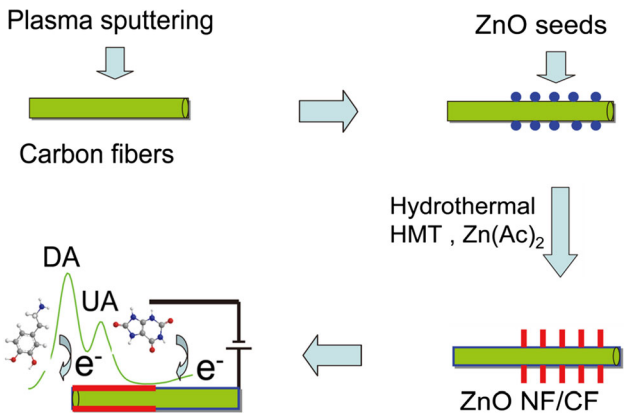

Scheme 1 Schematic diagram of ZnO NF/CF preparation and sensor assembly.

hydrothermally treated at 90 °C for 3 h and then to room temperature. Finally, ultra-long ZnO NF/CF was rinsed with deionized water and dried under vacuum at 60 °C for 6 h and used to detect UA and DA. The optimization of the morphologies and cross-sections of ZnO NF/CF is shown in Support Information Figs. S1–S4.

Results and discussion

Characterization of ultra-long ZnO NF/CF electrode

Here, ZnO is in situ hydrothermally grown on the carbon nanofiber to form a stand-by electrode. Figure 1a, b shows the typical structure of ZnO NF/CF. It can be seen that the material prepared by this method has an ordered orientation, and the ZnO on the surface of the carbon fiber is needle-like (Fig. 1b). This needle-like ZnO is uniform and covers the entire surface of each carbon fiber and is not aggregated (Fig. 1c). Further, the single ZnO has a diameter of about 18 nm and a length of 4.5 μm (Fig. 1d). The components of these prepared materials are mainly O, C, and Zn (Fig. 1e). Further component analysis is shown in the XRD diagram (Fig. 1f), where the 2θ = 26.5 and the 44° peak is assigned to (002) and (100) of the carbon fiber. Other results show a hexagonal wurtzite ZnO structure with no characteristic peaks of other impurities, indicating that the composition of the above nanofibers is ZnO and carbon fiber. Therefore, these results indicate that the nanocomposites are ZnO NF/CF. It is worth noting that the topography of the resulting sample of Fig. 1 shows that the needle-like ZnO nanolayer is uniform and orderly sputtered on the carbon nanofiber, which increases the specific surface area of the electrode and enhances the electron transport rate [3–5]. So, it can be expected that the *as*-prepared materials are competitive for the electrochemical applied.

Redox of UA or DA on ZnO NF/CF electrode

Figure S5 shows the cyclic voltammogram of the different electrodes. On the bare carbon fiber electrode, a weak oxidation peak of 0.4 V was observed and there was almost no reduction peak, which may be the hydrophobicity and chemical inertness of carbon fibers [25]. In contrast, a large oxidation current on the ZnO NF/CF electrode may be caused by several factors: (1) The central carbon fiber provides a channel for rapid electron transport; (2) the ZnO is a graphite-like structure [26], which forms a synergistic effect between ZnO and carbon fiber, and (3) the ZnO microstructure on the prepared ZnO/CF material is well dispersed, making UA easy to access conductive carbon fiber. In addition, ZnO/carbon fiber

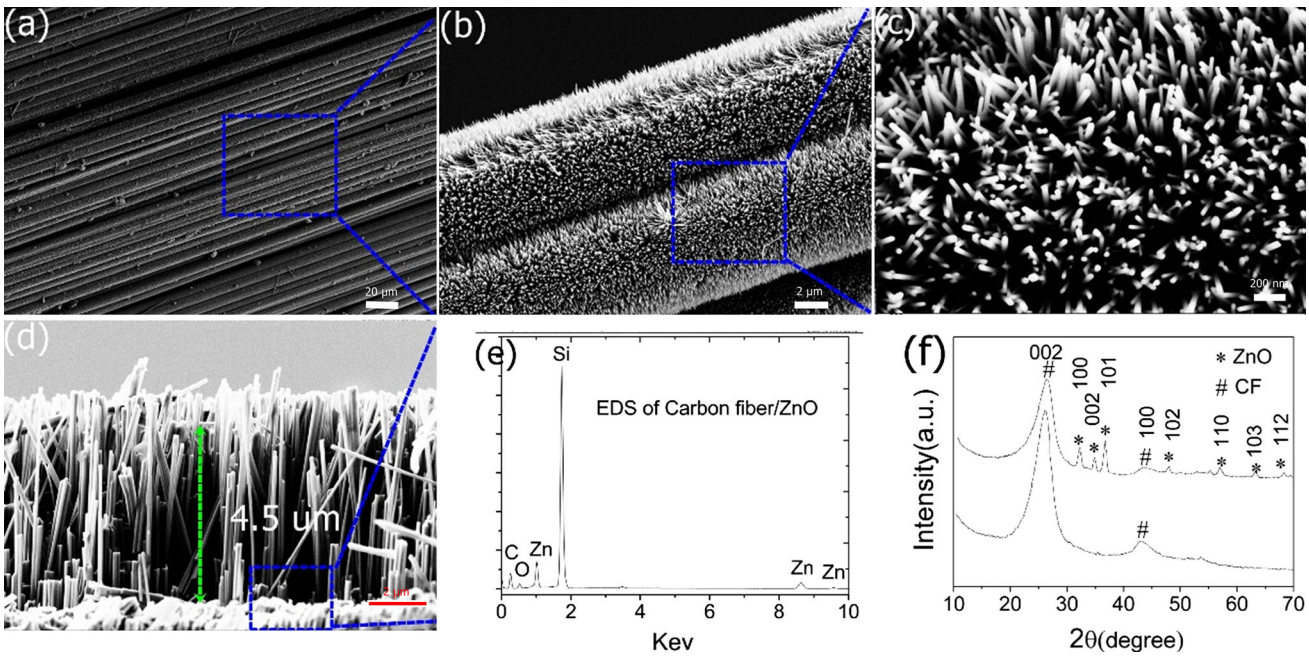

Figure 1 **a**–**c** Morphology with different magnifications, **d** length, **e** EDS, and **f** XRD of ultra-long ZnO NF/CF.

heterojunctions result in higher electrochemical activity [24]. For DA redox, there are similarities to UA, except for their oxidation potential [27, 28] (Fig. 2a). In addition, the chemical processes of UA and DA on the surface of the electrode are all oxidation processes controlled by surface diffusion (Fig. S6).

The electrical signal detection on the ZnO NF/CF electrode for UA or DA could be affected by electron transfer from the ZnO surface, as well as the electrolyte acidity, scan rate, and analyte concentration. As shown in Scheme 2, in the outermost layer of the ZnO crystal, there are many exposed zinc atoms, each of which has one or two free unoccupied empty orbitals [30]. Meanwhile, the valence electron orbitals of the oxygen atoms in the phenolic hydroxyl groups of DA and UA are sp^2 hybrid, and the lone pair electrons can be bonded to the upper orbital of Zn. In the electrochemical oxidation process, first, DA and UA molecules are adsorbed on the surface of the electrode. The unshared pair of oxygen atoms in the phenolic hydroxyl group is close to the unoccupied orbital of the zinc atom, and then, the compound is formed by orbital overlap. Since electrons are shared with zinc atoms, the electron density of oxygen atoms is lowered. The bond polarity of "OH" is increased, and H^+ can make DA and UA molecules as free positive ions. At the electrode voltage, the electrons in the coordinate-like will shift and transfer to the electrode. Then, a coordinate-like bond is broken, and the oxygen atom of the organic compound that loses hydrogen and two electrons will be positively charged, and thus, the electron cloud of the oxygen atom will deviate. For DA, the other hydrogens on the phenolic hydroxyl group will leave as H^+ and the large π bond of the benzene ring will be destroyed. Finally, a new π bond is formed between oxygen and carbon to produce o-benzoquinone. For UA, the hydrogen on the imidazole ring will leave as H^+ and produce a new conjugated molecule called ninhydrin.

DPV behavior of DA in the presence of UA

DPV is used here to detect DA and UA because it has higher sensitivity and better resolution than cyclic voltammetry [29]. The results of different concentrations of UA and DA are shown in Fig. 2a, b. Three important characteristics that must be considered are as follows: (1) Different oxidation potentials (0.35 V UA and 0.2 V DA) were observed, and (2) as the concentration increases, the oxidation current

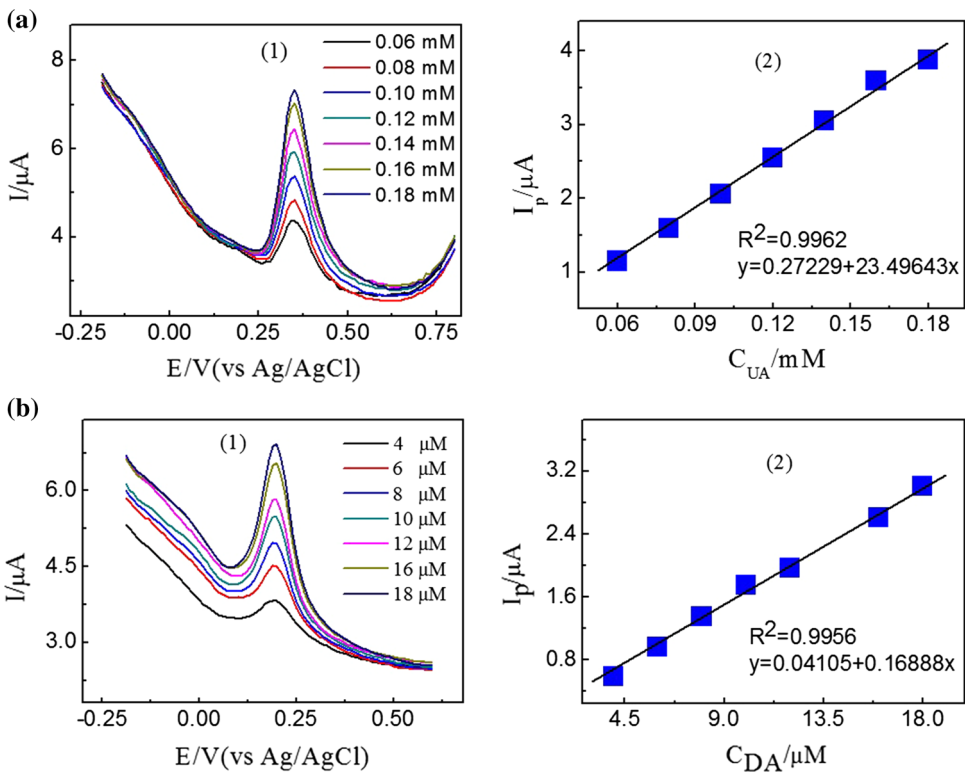

Figure 2 DPV electrochemical response (1) and linear range (2) of **a** DA and **b** UA on the ZnO NF/CF electrode.

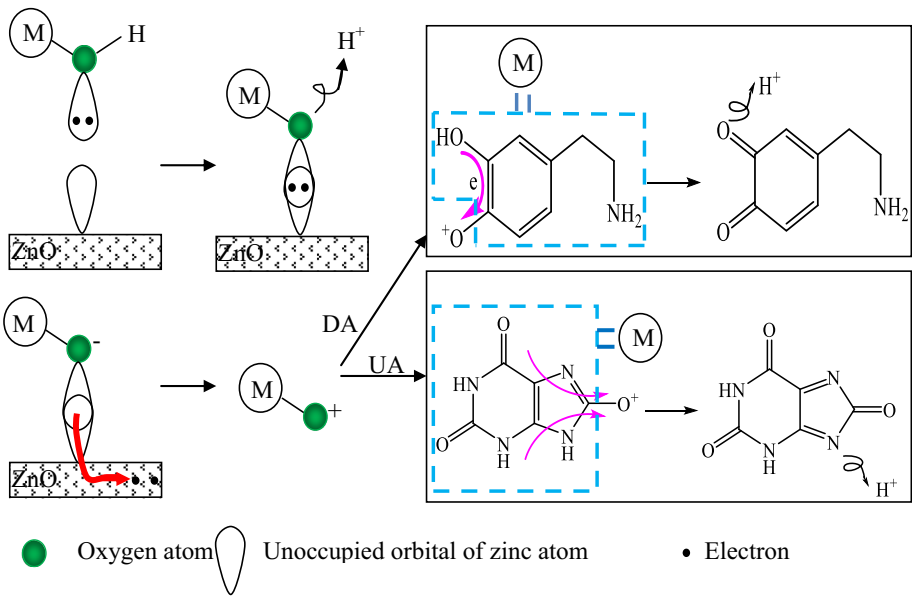

Scheme 2 Proposed mechanism of the oxidation process of DA and UA on the surface of ZnO NF/CF.

increases linearly, indicating a linear trajectory of UA and DA; (3) the oxidation current is affected by the adsorption force. UA and DA have aromatic rings in their molecular structure (Fig. S7), resulting in high oxidation currents (Fig. 2a, b). In addition, the specificity of such electrodes also shows better acceptability. The presence of glucose, potassium chloride, and sodium chloride did not affect the detection of UA or DA (Fig. S8).

For the electrochemical detection of the mixture of UA and DA, we changed the concentration of DA therein, while the concentration of UA was constant. As shown in Fig. 3, the DA concentration varied between 6 and 20 μM and the UA was fixed at a relatively large concentration of 0.1 mM. When the DA concentration increases, the oxidation peak current of DA also increases, but the oxidation peak current of UA is always constant. The peak potential of DA is 0.19, and the peak potential of UA is 0.38, which separates DA and UA well. The DA detection here has a linear range of 6–20 μM and a detection limit of ~ 0.402 μM, which is even better than some complex sensor results (see Table 1 for more information). These results also indicate that the ZnO NF/CF electrode can be used for the quantitative detection of DA in the coexistence of UA. Therefore, the ZnO NF/CF electrode is also a promising candidate for the selective determination of DA in the presence of UA.

Conclusion

In summary, the ZnO seed layer was successfully sputtered on carbon fiber by magnetron sputtering to prepare ultra-long ZnO NF/CF and directly used as a free-standing electrode. The electrode was

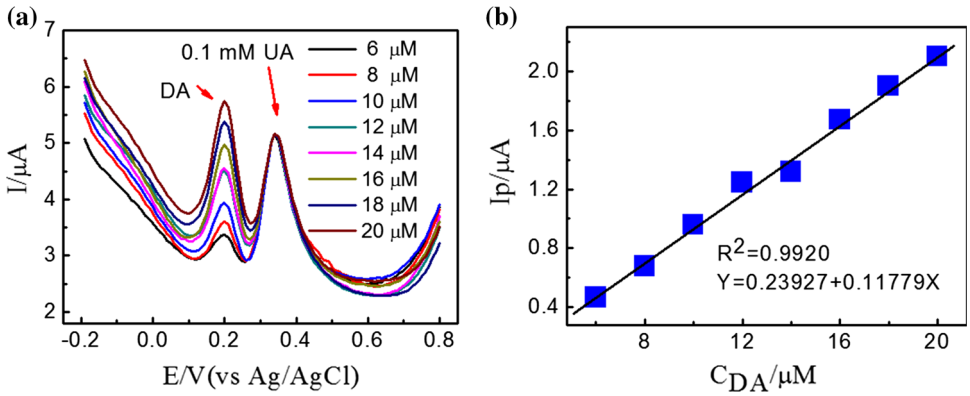

Figure 3 **a** DPV of DA with different concentrations containing 0.1 mM UA. **b** The corresponding plots of peak current versus the concentration of DA.

Table 1 UA and DA by DPV using different electrodes

Electrode	Sensitivity (linear range) (μA/μM)	
	UA	DA
TCPP/CCG/GCE [30]	–	1.4 (0.01–70)
PS/GP/GCE [31]	–	1.99 (0.1–0.9)
ZnONPs/CPE [32]	–	3.54 (0.1–20)
Pd/Fe_3O_4/GCE [1]	–	0.04 (0.96–107)
NiO/ZnO/CPE [33]	0.035 (12.9–629)	1.78 (1–6)
	0.001 (629–6290)	0.14 (6–100)
Au-NCs [2]	– (0.7–80)	–
GC-ERGO [34]	8.47 (0.1–10)	–
H-G/S/GCE [5]	4.56 (2.5–65)	–
GQD-Ce(IV) [16]	– (1–500)	–
This work	(60–180)	(4–20)

characterized, and the electrochemical processes of UA and DA on the electrode surface were discussed. The DPV method can be used to detect sensitive DA or UA, and the detection of DA can be realized under the high concentration of UA (0.1 mM). The DA detection here has a linear range of 6–20 μM and a detection limit of ~ 0.402 μM. These results indicate that this electrode can perform effective electrochemical oxidation of UA and DA and the resolution of oxidation peaks and can be used as an alternative for the simultaneous detection of UA and DA.

Funding

This work was supported by the National Natural Science Foundation of China (Grant Nos. 91644103, 41603104, 61404075), the National Key Research and Development Program of China (2017YFC0212302), the Postdoctoral Foundation of Jiangsu Province (1601090B), the China Postdoctoral Science Foundation (2016M601694), and the Natural Science Foundation for Young Scientists of Jiangsu Province, China (BK20150895). Also including the Program for Changjiang Scholars and Innovative Research Team in University of Ministry of Education of China (PCSIRT) and the Priority Academic Program Development of Jiangsu Higher Education Institutions (PAPD). At the same time, we also thank Professor Yanlin Zhang for his support and discussion.

Compliance with ethical standards

Conflict of interest All the authors have declared that: (1) no support, financial or otherwise, has been received from any organization that may have an interest in the submitted work, and (2) there are no other relationships or activities that could appear to have influenced the submitted work.

Electronic supplementary material: The online version of this article (https://doi.org/10.1007/s10853-019-04000-x) contains supplementary material, which is available to authorized users.

References

[1] Iijima S (1991) Helical microtubules of graphitic carbon. Nature 354(6348):56–58

[2] Kong J, Franklin NR, Zhou C, Chapline MG, Peng S, Cho K, Dai H (2000) Nanotube molecular wires as chemical sensors. Science 287(5453):622–625

[3] Yang C, Gu B, Zhang D, Ge C, Tao H (2016) Coaxial carbon fiber/ZnO nanorods as electrodes for the electrochemical determination of dopamine. Anal Methods 8(3):650–655

[4] Ahmad M, Pan C, Luo Z, Jing Z (2010) A single ZnO nanofiber-based highly sensitive amperometric glucose biosensor. J Phys Chem 114(20):9308–9313

[5] Katoch A, Sun GJ, Choi SW, Byun JH, Sang SK (2013) Competitive influence of grain size and crystallinity on gas sensing performances of ZnO nanofibers. Sens Actuators B Chem 185(8):411–416

[6] Zhang Z, Li X, Wang C, Wei L, Liu Y, Shao C (2009) ZnO hollow nanofibers: fabrication from facile single capillary electrospinning and applications in gas sensors. J Phys Chem C 113(45):19397–19403

[7] Lin D, Hui W, Rui Z, Wei P (2009) Enhanced photocatalysis of electrospun Ag–ZnO heterostructured nanofibers. Chem Mater 21(15):3479–3484

[8] Gu B, Zhong L, Wang X, Dong X (2016) RF magnetron sputtering synthesis of carbon fibers/ZnO coaxial nanocable microelectrode for electrochemical sensing of ascorbic acid. Mater Lett 181:265–267

[9] Wang S, Xia L, Yu L, Zhang L, Wang H, Lou XW (2016) Free-standing nitrogen-doped carbon nanofiber films: integrated electrodes for sodium-ion batteries with ultralong cycle life and superior rate capability. Adv Energy Mater 6(7):1502217

[10] Chen C, Li D, Hu Q, Wang R (2014) Properties of polymethyl methacrylate-based nanocomposites: reinforced with

ultra-long chitin nanofiber extracted from crab shells. Mater Des 56:1049–1056

[11] Jie F, Dan L, Huang J, Chao Z, Xiao D, Zhang L (2018) Growth of aligned ZnO nanorods on carbon fabric and its composite for superior mechanical and tribological performance. Surf Coat Technol 344:433–440

[12] Zhang J, Han D, Yang RQ, Ji YC, Liu J, Yu L (2019) Electrochemical detection of DNA hybridization based on three-dimensional ZnO nanowires/graphite hybrid microfiber structure. Bioelectrochemistry 128:126–132

[13] Smith SK, Gosrani SP, Lee CA, McCarty GS, Sombers LA (2018) Carbon-fiber microbiosensor for monitoring rapid lactate fluctuations in brain tissue using fast-scan cyclic voltammetry. Anal Chem 90(21):12994–12999

[14] Zhang J, Han D, Wang S, Zhang XD, Yang RQ, Ji YC, Yu X (2019) Electrochemical detection of adenine and guanine using a three-dimensional WS_2 nanosheet/graphite microfiber hybrid electrode. Electrochem Commun 99:75–80

[15] Sun YL, Lin YL, Han R, Wang XY, Luo CN (2019) A chemiluminescence biosensor for lysozyme detection based on aptamers and hemin/G-quadruplex DNAzyme modified sandwich-rod carbon fiber composite. Talanta 200:57–66

[16] Liu H, Gu C, Hou C, Yin Z, Fan K, Zhang M (2016) Plasma-assisted synthesis of carbon fibers/ZnO core–shell hybrids on carbon fiber templates for detection of ascorbic acid and uric acid. Sens Actuators B Chem 224:857–862

[17] Sun C-L, Chang C-T, Lee H-H, Zhou J, Wang J, Sham T-K, Pong W-F (2011) Microwave-assisted synthesis of a core–shell MWCNT/GONR heterostructure for the electrochemical detection of ascorbic acid, dopamine, and uric acid. ACS Nano 5(10):7788–7795

[18] Lavoie MJ, Ostaszewski BA, Schlossmacher MG, Selkoe DJ (2005) Dopamine covalently modifies and functionally inactivates parkin. Nat Med 11(11):1214

[19] Ghoreishi SM, Behpour M, Fard MHM (2012) Electrochemical methods for simultaneous determination of trace amounts of dopamine and uric acid using a carbon paste electrode incorporated with multi-wall carbon nanotubes and modified with α-cyclodextrine. J Solid State Electrochem 16(1):179–189

[20] Jian T, Zhang L, Yun L, Jie Z, Han G, Tang W (2015) Gold nanoparticles-β-cyclodextrin-chitosan-graphene modified glassy carbon electrode for ultrasensitive detection of dopamine and uric acid. Electroanalysis 26(9):2057–2064

[21] Vinoth V, Wu JJ, Anandan S (2016) Sensitive electrochemical determination of dopamine and uric acid using AuNPs(EDAS)–rGO nanocomposites. Anal Methods 8(22):4379–4390

[22] Jie C, Han X, Sun H, Shao S, Weng L, Wang L (2016) Platinum nanoparticles supported MoS_2 nanosheet for simultaneous detection of dopamine and uric acid. Sci China Chem 59(3):332–337

[23] Yang L, Pei S, Jin G, Wu W, Xu S, Li J, Kang Z, Deng A (2015) A novel sensor based on electrodeposited Au–Pt bimetallic nano-clusters decorated on graphene oxide (GO)–electrochemically reduced GO for sensitive detection of dopamine and uric acid. Sens Actuators B Chem 221:1542–1553

[24] Wang J, Yang B, Zhong J, Yan B, Zhang K, Zhai C, Shiraishi Y, Du Y, Yang P (2017) Dopamine and uric acid electrochemical sensor based on a glassy carbon electrode modified with cubic Pd and reduced graphene oxide nanocomposite. J Colloid Interface Sci 497:172–180

[25] Khan AF, Brownson DAC, Randviir EP, Smith GC, Banks CE (2016) 2D hexagonal boron nitride (2D-HBN) explored for the electrochemical sensing of dopamine. Anal Chem 88(19):9729–9737

[26] Khan MMI, Baek GW, Kim K, Kwon HI, Jin SH (2017) Simultaneous detection of dopamine and uric acid on indium tin oxides modified with cost-effective gas-phase synthesized single walled carbon nanotubes. Electroanalysis 29(8):1925–1933

[27] Wang D, Huang B, Liu J, Guo X, Abudukeyoumu G, Zhang Y, Ye B-C, Li Y (2018) A novel electrochemical sensor based on Cu@ Ni/MWCNTs nanocomposite for simultaneous determination of guanine and adenine. Biosens Bioelectron 102:389–395

[28] Baig N, Kawde AN, Ibrahim M (2019) A new approach of controlled single step in situ fabrication of graphene composite sensor for simultaneous sensing of small biomolecules in human urine. ChemistrySelect 4(5):1640–1649

[29] Alipour E, Majidi MR, Saadatirad A, Mahdi Golabi S, Alizadeh AM (2013) Simultaneous determination of dopamine and uric acid in biological samples on the pretreated pencil graphite electrode. Electrochim Acta 91:36–42

[30] Tatsuma T, Watanabe T (1991) Oxidase/peroxidase bilayer-modified electrodes as sensors for lactate, pyruvate, cholesterol and uric acid. Anal Chim Acta 242:85–89

[31] Guan Y, Wu T, Ye J (2005) Determination of uric acid and *p*-aminohippuric acid in human saliva and urine using capillary electrophoresis with electrochemical detection: Potential application in fast diagnosis of renal disease. J Chromatogr B 821(2):229–234

[32] Ross MA (1994) Determination of ascorbic acid and uric acid in plasma by high-performance liquid chromatography. J Chromatogr B Biomed Sci Appl 657(1):197–200

[33] Dutt JSN, Cardosi MF, Livingstone C, Davis J (2005) Diagnostic implications of uric acid in electroanalytical measurements. Electroanal Int J Devoted Fundam Pract Asp Electroanal 17(14):1233–1243

[34] Hermanson KD, Lumsdon SO, Williams JP, Kaler EW, Velev OD (2001) Dielectrophoretic assembly of electrically functional microwires from nanoparticle suspensions. Science 294(5544):1082–1086